UPPSALA
UNIVERSITET

UPTEC ES 22034
Examensarbete 30 hp
November 2022

# Magnetron sputtering of transparent conducting tungsten doped indium oxide

Erica Evertsson

Fullständigt programnamn (t ex Civilingenjörsprogrammet i informationsteknologi)

UPPSALA UNIVERSITET

# Magnetron sputtering of transparent conducting tungsten doped indium oxide

Erica Evertsson

## Abstract

In thin film solar cells there is a front contact layer called TCO, transparent conducting oxide. This layer requires high conductivity and high transmittance. Different materials such as Tin doped indium oxide (ITO) and Aluminum doped zinc oxide (AZO) are current good alternatives but several other materials are investigated to find even better materials. One of them is tungsten doped indium oxide (IOW). This project was about investigating the deposition process for IOW and characterize the properties of IOW thin film to investigate the possibilities for implementing this material as a contact layer in thin film solar cells. The results from the two batches of depositions varied a lot. Some samples came out dark, but some were transparent and had a high transmittance, suitable for a TCO. The highest transmittance reached through this process was around 95 % in the infrared (IR) range and around 90 % in the visible range. When it comes to the resistivity, no IOW-samples reaches desired levels for a TCO. The lowest resistivity reached was $6.36 * 10^{-4}$ Ω cm. The results showed that the sample with the lowest resistivity was the undoped material, which is contradicting the current theory on the subject. The lowest resistivity for the IOW film was $6.50 * 10^{-3}$ Ω cm.

**Teknisk-naturvetenskapliga fakulteten**

**Uppsala universitet, Utgivningsort Uppsala/Visby**

Handledare: Förnamn Efternamn  Ämnesgranskare: Förnamn Efternamn

Examinator: Förnamn Efternamn

Detta examensarbete är sekretessbelagt t o m Klicka och välj datum eller skriv i fältet. (Tas bort om ej sekretessbelagt)

# Populärvetenskaplig sammanfattning

Mot bakgrund av den pågående omställningen till förnybar energi pågår omfattande forskning kring alternativ till fossila energikällor. Ett av dessa är solenergi. Solceller har genom åren utvecklats i rasande fart och något som är väldigt aktuellt i forskarvärlden är tunnfilmssolceller. Tunnfilmssolceller förlitar sig på att ha kontaktskikt med lämpliga egenskaper. Det yttersta lagret på solceller, framkontakten, måste vara transparent och samtidigt ledande. Bland de material som uppfyller dessa motstridiga krav finns transparent ledande oxid (TCO på engelska). Dagens TCO:er är främst baserade på tenndioxid ($SnO_2$), indiumoxid ($In_2O_3$) eller zinkoxid (ZnO). Indiumtennoxid (ITO) är en enastående ledare som kombinerar utmärkta elektriska egenskaper med god kemisk stabilitet. Aluminiumdopad zinkoxid (AZO) är ett annat vanligt och billigare alternativ med konduktivitet som når ITO [1]. Det nuvarande intresset för tandemsolceller, där olika solceller kombineras genom olika lager för att öka verkningsgraden, ökar behovet av ännu bättre material, med högre transmittans utan att offra elektrisk ledningsförmåga. Därför undersöks nu alternativ till TCO. En av dessa är vätedopad indiumoxid. Den har utmärkta prestandaegenskaper som överstiger indiumtennoxid (ITO), men processen är komplicerad eftersom vatten används under tillväxten. Ett annat möjligt alternativ kan därför vara volframdopad indiumoxid, IOW. Enligt litteraturen kan IOW erbjuda låg resistivitet, i storleksordningen $10^{-4}$ Ωcm (odopad ligger runt $10^{-3}$- $10^{-4}$ Ωcm [2]). De optiska egenskaperna är också lämpliga för ett TCO-lager och kemisk stabilitet [3].

I detta projekt undersöktes volframdopad indiumoxid som en alternativ TCO. Detta gjordes genom att belägga en bit glas med detta material, genom en metod som kallas sputtring. I en sputterprocess skapas ett plasma i en argongas med hjälp av magnetroner som accelererar elektroner. Elektronerna överför sin energi till argonatomer som slår ut elektroner, vilket gör argonatomerna joniserade (plus-laddade) och skapar plasmat. De positiva jonerna accelereras mot det material som man vill belägga, i det här fallet indiumoxid och volfram, och överför sin energi till materialet. Därmed slås atomer ut från ytan och kan fångas upp på det prov som man vill belägga [4]. Under sputtringsprocessen varierades mängden syre och mängden volfram i proverna för att undersöka skillnader i ledningsförmåga och optiska egenskaper.

Mätningar som gjordes på proverna var optiska mätningar: transmittans, reflektans och absorption, det vill säga hur mycket ljus proverna släpper igenom, respektive reflekterar och absorberar. Även mätningar med 4-punkts prob och profilometer gjordes för att få ut resistivitet för de olika proverna och på så sätt jämföra ledningsförmåga. Med 4-punkts proben mäts ytresistansen på tunnfilmen och tillsammans med mätningar från profilometer, som mäter tjockleken, fås resistiviteten.

Resultaten var varierade och avvek från de resultat som kunde förväntas enligt litteraturen. Några prover blev väldigt mörka vilket bidrog till en låg transmittans. Andra prover var väldigt transparenta och hade hög transmittans, men uppnådde inte önskvärd resistivitet för att prestera som ett TCO. Den lägsta resistiviteten som uppnåddes var $6.36 \cdot 10^{-4}$ Ωcm och var för det odopade materialet, vilket inte stämmer överens med litteraturen, som säger att wolframdopning ska ge lägre

resistivitet än odopad $In_2O_3$ [3].

Utifrån resultaten från detta projekt så lämpar sig inte IOW som ett TCO i tunnfilmssolceller på grund av den för höga resistiviteten. Däremot har materialet hög transmittans. Fortsatta analyser som kunde gjorts av proverna var att se om värmebehandling skulle kunna öka ledningsförmågan och därmed förbättra IWO-proverna.

# Executive summary

The aim of this project was to investigate the deposition process for IOW and characterize properties of IOW thin films to then analyze the results and explain the observed behaviour and to see if the material qualifies as a good transparent conducting oxide (TCO).

The IOW films were deposited by Radio Frequency (RF) magnetron sputtering. In the first batch of depositions the goal was to find out what impact the oxygen gas flow level and tungsten concentration in the sputtering process had on the outcome, with regard to transmittance and resisitivity. This was done by first varying the oxygen gas flow level until an optimal flow was found. After the optimal oxygen gas flow level had been found, the tungsten concentration was varied for the remaining samples in the batch. The samples were characterized by measuring the resistivity and optical properties. After analyzing the results, another batch of depositions was made based on the results in the first batch.

The results from the two batches varied a lot. Some were dark and therefore not a good TCO but some had a high transmittance. The highest transmittance reached through this process was around 95 % in the IR range and around 90 % in the visible range. When it comes to the resistivity, no IOW-samples reaches desired levels for a TCO. The results show that the material with the lowest resistivity was the undoped material, with an achieved resistivity of $6.36 \cdot 10^{-4}$ $\Omega$. This is contradicting the current theory on the subject, which states that tungsten doping should give lower resistivity than undoped $In_2O_3$ [3].

# Acknowledgements

This project was the last step in my master of science engineering in energy systems at Uppsala University. I would like give my sincerest thanks to my supervisor Tomas Kubart and my subject reviewer Tobias Törndahl for being a great support throughout the project and always providing me with a lot of help. I would also like to thank other employees at the two departments I have worked with for the commitment and involvement in my project. Last but not least I would like to thank my boyfriend, family and friends for helping me in the writing process and being a mental support throughout this period of time.

*Uppsala, October 2022*
*Erica Evertsson*

# Contents

**List of Abbreviations** **vi**

**1 Introduction** **1**
1.1 Background . . . 1
1.2 Aim of this project . . . 1
1.3 Literature review . . . 1

**2 Theory** **3**
2.1 Transparent conducting oxide (TCO) and applications . . . 3
2.2 Magnetron sputtering deposition . . . 4

**3 Method** **6**
3.1 Deposition process . . . 6
3.2 Sample preparation . . . 6
3.3 First batch of depositions . . . 6
3.4 Second batch of depositions . . . 7
3.5 Characterization methods . . . 7
3.5.1 Spectrophotometer . . . 7
3.5.2 4-point probe . . . 8
3.5.3 Profilometer . . . 8
3.5.4 XRF . . . 9
3.5.5 XRD . . . 9
3.5.6 GDOES . . . 10
3.5.7 SEM . . . 10

**4 Results & Discussion** **11**
4.1 First batch of depositions . . . 11
4.2 Second batch of depositions . . . 19
4.3 Suggested improvements . . . 25

**5 Conclusion** **26**

**6 Appendix** **28**

# List of Abbreviations

**AZO** Aluminum doped zinc oxide

**IOW** Tungsten doped indium oxide

**IPA** Isopropyl alcohol

**ITO** Tin doped indium oxide

**RF** Radio Frequency

**SEM** Scanning electron microspope

**TCO** Transparent Conducting Oxide

**XRD** X-ray Diffraction

**XRF** X-ray Fluorescence

# 1 Introduction

## 1.1 Background

In the current situation, with the transition to renewable energy, extensive research is taking place on alternatives to the fossil energy sources. One such alternative energy source is solar energy. Over the years, solar cells have developed at breakneck speed and a topic that is very relevant to the research area of solar cells is the topic of thin film solar cells.

Optoelectronic devices, including thin film solar cells, rely on suitable contact layers. In many cases, such as the front contact on a solar cell, this contact layer has to be transparent and at the same time conductive. Among the materials that fulfill these conflicting requirements, transparent conducting oxide (TCO) are prominent. Present TCOs are based on three binary oxides, $SnO_2$, $In_2O_3$, or ZnO. Indium tin oxide (ITO) is an outstanding conductor which combines excellent electrical properties with good chemical stability. Aluminium doped zinc oxide (AZO) is a common lower cost alternative with conductivity reaching that of ITO [1]. Current interest in tandem solar cells, where different solar cells are combined through different layers to increase efficiency, brings the need for even better materials, with higher transmittance without sacrificing electrical conductivity. Therefore, an alternative TCO, H-doped indium oxide has been investigated. It has excellent performance exceeding that of ITO, however, $H_2O$ is required to synthesize H-doped indium oxide making the synthesization process more complicated [5]. Another possible alternative might be tungsten-doped indium oxide, IOW. According to the literature, IOW might offer low resistivity on the order of $10^{-4}$ Ωcm. The optical performances are also suitable for a TCO layer [3].

## 1.2 Aim of this project

This project investigates the feasibility of tungsten indium oxide as a TCO in solar cells. The goal is to replace existing materials such as AZO or ITO with an alternative that offers the same electrical conductivity with improved transmittance.

Specific aims:

- Investigate deposition process for IOW
- Characterize properties of IOW thin films
- Analyze the results and explain the observed behaviour

## 1.3 Literature review

Different scientific articles were reviewed to collect knowledge about previous studies about tungsten doped indium oxide (IOW). In particular the parameters analyzed were resistivity and transmittance to compare the values from literature to the ones in this project. In general, the characteristics of a good material suitable to perform as TCO can be compared with the current used material ITO. In that case the resistivity should be on the order of $10^{-4}$ Ωcm and the transmittance above 90 % of the light in the visible region [1].

The articles that were reviewed, deal all with IOW but synthesized by different methods. The results turned out to be very similar when comparing each article. The resistivity in all of the studies were in the size of around $10^{-4}$ Ωcm while the transmittance was around 80 - 90 %. These values serves as reference values when comparing the samples in this project. The studies varied different parameters. Some varied tungsten content [6], other investigated the effect of growth temperature [7] and another one varied oxygen pressure [8].

When varying tungsten content, the results showed that a tungsten content of around 3 wt% gave the lowest resistivity. Also, more tungsten both leads to higher resistivity and negatively affected transmittance. The carrier concentration of IOW films is much higher than that of undoped $In_2O_3$ films and is also growing initially when increasing the amount of W-doping content but decreases with further increasing of W-doping content [6].

For an excessively high sputtering power (higher than 50 W), incomplete oxidation might cause a large number of defects, and the clubbed nano-wire monocrystallines are loosely arranged, causing increased grain boundary scattering and leading to reduced carrier mobility [9].

When the substrate temperature is varied, an increase in temperature led to decrease in resistivity [7]. If the thin films are polycrystalline, heating or annealing above 250 °C is needed for the deposition to improve the electrical properties [3].

The variation of oxygen pressure showed that increasing oxygen pressure during film deposition, decreases the number of oxygen vacancies in the films, which leads to decrease in carrier concentration and concomitantly to an increase in film resistivity [8].

In summary, both the electrical properties and optical transparency of the films depend on growth temperature and oxygen pressure. The growth temperature and the oxygen pressure in the chamber play a significant role in obtaining high mobility film and therefore high conductivity [8].

# 2 Theory

In this section, all theory, tools and equations used in the project are described.

## 2.1 Transparent conducting oxide (TCO) and applications

Transparent conducting oxide, TCO, is an oxide that has the unique combination of being electrically conductive and optically transparent. Such materials are used in optoelectronic devices, for example photovoltaic (Figure 1 illustrates where TCO is placed in a thin film solar cell). Simultaneously achieving electrical conductivity and high transmittance is not trivial. The studied TCO in in this project was indium oxide, a transparent, wide band gap (around 3 eV) semiconductor, doped with tungsten for conductivity. The optical properties of indium oxide are suitable for a TCO, as the material is transparent and has low absorption. In TCOs, the optical band gap is larger than 3.2 eV. This lies in the ultraviolet region and therefore TCOs does not absorb visible light, and appears to be transparent. The microstructures in these films are mostly polycrystalline or amorphous. By being polycrystalline means that the material consists of several crystalline parts, randomly oriented in the material. Amorphous means there is no clear structure, like in crystals. The main properties of TCOs are high transmittance (above 90 % for incident light) and high conductivity (higher than $10^3$ per Ωcm). ITO and AZO are two types of material suitable for a TCO. ITO has a transmittance above 90 % in the visible region and a resistivity in the size of $10^{-4}$ Ωcm. AZO has the same size of resistivity but a slightly lower transmittance (around 80 - 85 %) [1]. When TCO should be used in solar cell other parameters like carrier concentration and mobility are interesting to measure.

If a TCO should be suitable for most electrode applications, the charge carrier mobility need to be maximized ($\mu = 50$ - 70 $\text{cm}^2\text{V}^{-1}\text{s}^{-1}$) and the electrical resistivity minimized ($\rho$ = $10^{-4}$ - $10^{-5}$ Ω cm). At the same time you want to minimise undesired optical absorption by keeping the carrier concentration below $2 \cdot 10^{21}$ $\text{cm}^{-3}$ [1].

The mobility describes the charge carrier's ability to move through its crystal lattice. The conductivity of a TCO is directly related to the number of charge carriers and their mobility. This is linerarly related by the Boltzmann formulation in equation 1.

$$\sigma = qn\mu \tag{1}$$

where $\sigma$ is the electrical conductivity in $\text{Scm}^{-1}$, $q$ is the elementary charge ($1.602 \cdot 10^{-19}$), $n$ is the charge carrier density and $\mu$ is the electron mobility. With equation 1 it is easy to see that to increase the conductivity the charge carrier density has to increase, but also the carrier mobility could be increased to improve the conductivity. Even though it is possible to tune the mobility it is strongly connected to the material used and thus making the carrier concentration, through doping, the property of choice when tuning the conductivity. The mobility should, however, not be forgotten as it is crucial to have a good mobility when striving for a high conductivity and a high transparency [1].

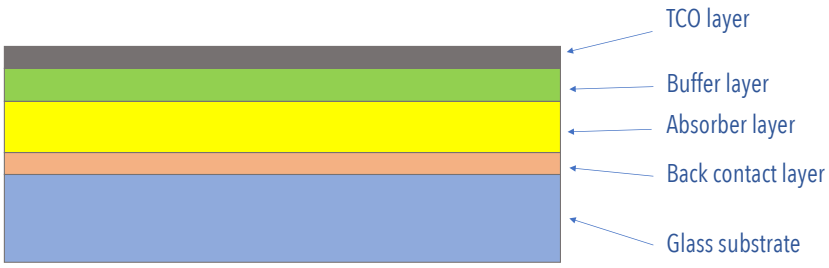


Figure 1: A typical CIGS thin film solar cell structure.

## 2.2 Magnetron sputtering deposition

To synthesize the thin films, magnetron sputtering was used. Magnetron sputtering is a physical vapor deposition technique that uses a solid piece of the material to deposite, i.e. the *sputtering target*, that is converted to vapor by ion bombardment. The vapor then condenses on a surface to be coated. The process takes place at a low pressure and an electric discharge is used to create a plasma that supplies the ions [4].The method is illustrated in figure 2.

In magnetron sputtering, a magnetic field is applied to the sputtering target to trap electrons in the target vicinity. This way, a denser plasma is created and the ion current density is increased as compared to a diode discharge. The magnetic field is most often created by a system of permanent magnets placed behind the sputtering target. A high negative voltage, several 100s V, is applied to the target. The magnetic field strength is such that electrons are trapped while ions are not affected.

In the discharge, electrons are emitted from the sputtering target. The electrons are accelerated in the applied electric field and collide with the argon gas and ionize it. The collision leads to a positive argon ion that attracts to the negative voltage on the target and the ion accelerates towards the target and collide with target atoms and some of the atoms may be "kicked out", sputtered, from the target surface. These atoms condense on the substrate.

The magnetron source is placed in a vacuum chamber. The flow of argon gas and its pressure, discharge voltage, as well as possible $O_2$ addition are process parameters that can be controlled. In this work, two magnetron sources were used, one with $In_2O_3$ and another with W sputtering target. By adjusting the discharge power on

the W source, the content of W can be varied to reach desired performances [4].

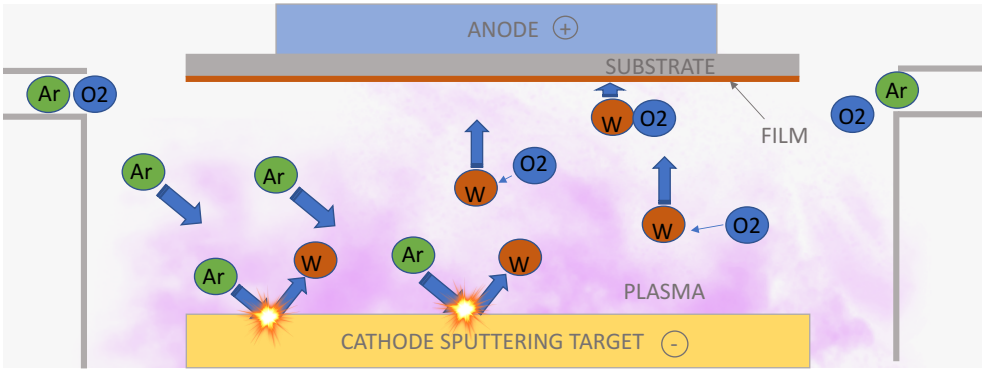


Figure 2: Sputter deposition.

# 3 Method

## 3.1 Deposition process

In this project two batches of depositions were made. Glass substrates were coated with tungsten doped indium oxide by radio frequency (RF) magnetron co-sputtering. In the sputter there were one metal target with tungsten and one ceramic target with indium oxide. Therefore, RF was used to sputter the electrically insulating indium oxide target while tungsten was sputtered using direct current (DC). The distance between the target and substrate was 180 mm. The base pressure in the first batch was $3 \cdot 10^{-6}$ Torr and $3 \cdot 10^{-7}$ Torr in the second batch. The working pressure was 5 mTorr for both batches. Indium was sputtered with a voltage of around 240 V and power of 280 W. The substrate was deposited without intentional heating. In the process, the concentration of tungsten was varied by changing the tungsten sputtering power, and also the oxygen gas flow. These samples were then characterized through different measurements described later in this section.

## 3.2 Sample preparation

The substrates used in every deposition were 2.5x5 cm quartz and soda-lime glass, plus a small piece of silicon. The quartz glass substrates were first washed using ultrasonic cleaning. The glass was put in a beaker. The beaker was filled with isopropyl alcohol (IPA) to cover the glass. Then the glass was washed for 5 minutes in the ultrasonic bath and then cleaned in deionized water. The soda-lime glass was covered with a small piece of kapton tape, to have an area without deposition for measuring film thickness with profilometry. In the sputter, the substrates were placed in the same place for all depositions to avoid the small risk of differences that might be depending on where the substrate is placed in the chamber.

## 3.3 First batch of depositions

In the first batch the oxygen gas flow was varied, with only indium oxide target, to find an optimal oxygen gas flow. The oxygen gas flow rates that were tested were 0.2, 0.3 and 0.5 sccm. Then, the tungsten was added to the process with varied sputtering power, while the oxygen gas flow was set due to previously found optimal gas flow rates. The different powers were 15 and 20 W in the first depositions with tungsten. After analyzing the results from these, a lower tungsten sputtering power than 15 W was more suitable to decrease resistivity. During the process different ways of introducing oxygen were tested, in an attempt to try to reduce the tungsten content. Oxygen was led directly to the tungsten target to oxidize it before sputtering. To reduce the tungsten content even more, a different way of powering the tungsten target was tested, pulsed magnetron sputtering. In this approach, pulses with a defined length and energy are applied. By adjusting the frequency, the average sputtering power can be controlled. In this case a frequency of 100 Hz was used with 30 $\mu$s pulses and 33 mJ/pulse [10]. This sputtering method was used for sample IOW16-IOW17 (See section 4). For these samples the average tungsten power was estimated to be 3 W, with two different oxygen gas flow, 0.3 and 0.5 sccm respectively. The resistivity was measured for all the samples using

the four-point probe and profilometer as described in the theory section. Some of the samples were further measured with spectrophotometer.

Since it could be determined only from the appearance that certain samples would not give good measurement results, no further measurements were made on these. A few of the samples were measured with XRF to get information about the tungsten to indium ratio in the films with different tungsten power. Also, a few samples were measured with XRD to see examples of the structure of the thin films, if differences in crystalline structures could be detected for varying tungsten content.

## 3.4 Second batch of depositions

In the second batch of depositions the process was optimized using the results from the first batch. Only three depositions were made in this batch using the optimized parameters determined from the previous batch. For the three samples, a constant flow of oxygen was chosen, 0.3 sccm and only the sputtering power of tungsten was varied by 0, 1.5 and 3 W. The oxygen flow was chosen from the results in the first batch. In this second batch the tungsten concentration was kept low using pulsed magnetron sputtering with the same parameters as in the first batch, except this time the frequency was varied. For IOW18 the frequency was 100 Hz and for IOW19 50 Hz, thus expecting reduced tungsten concentration compared to IOW18. The deposition without tungsten (IOW20) was sputtered using the same method and recipe as in the first batch when RF magnetron sputtering was used. All depositions were measured with four-point probe, profilometer, spectrophotometer and XRF. No XRD measurements were made on these samples since they were assumed to have the same structure.

## 3.5 Characterization methods

### 3.5.1 Spectrophotometer

A spectrophotometer was used to measure the optical properties. With a spectrophotometer you can measure the reflectance and transmittance for different wavelengths, and thus find out the absorptance. In the instrument there is a light source where the light passes through a small gap so only a thin strip of light passes to the other side. Behind the gap there is a rotatable prism to divide the light in different wavelengths. After the prism there is another gap where the light passes through to the sample you want to measure. There are two different positions to put your sample in to either measure how much light that passes through the sample, or how much light the sample reflects. From that you get the reflectance and transmittance of the material in percent. The relation between reflectance ($R$), transmittance ($T$) and absorptance ($A$) is shown in equation 2. Using that equation you can get absorptance for the material. [4].

$$A = 100\% - T - R \tag{2}$$

### 3.5.2 4-point probe

A four-point probe was used to measure sheet resistance ($R_s$) in the thin film material. The tool has four probes that touches the sample surface. The two outer probes measures electric current and the inner two measures voltage. The distance between the probes are the same. A constant electric current is streamed between the two outer probes along the thin film. There will be a voltage drop if there is a resistance in the material. This difference in voltage is measured through the inner probes and the measured current and voltage drop give the sheet resistance. The unit of sheet resistance is Ω/sq., which means the surface resistivity of any given square of the material. When you have measured the sheet resistance you can multiply it with the thickness of the thin film to get the resistivity of the thin film [11].

The resistivity $\rho$ of the thin film was calculated using equation 3 where $R_s$ is the sheet resistance measured with the four point probe, and $t$ is thickness of the thin film [11].

$$\rho = R_s \cdot t \tag{3}$$

### 3.5.3 Profilometer

A profilometer was used to measure thickness of the thin film by measuring the surface of the substrate. A stylus with a camera is moved across the surface of the substrate and measures dynamic changes in topography in real-time. Since a kapton tape was covering a part of the substrate during deposition that part was not deposited. The stylus is drawn over the surface without deposition and up to the surface with deposition, to measure that height. This height gives the film thickness (see figure 3) [4].

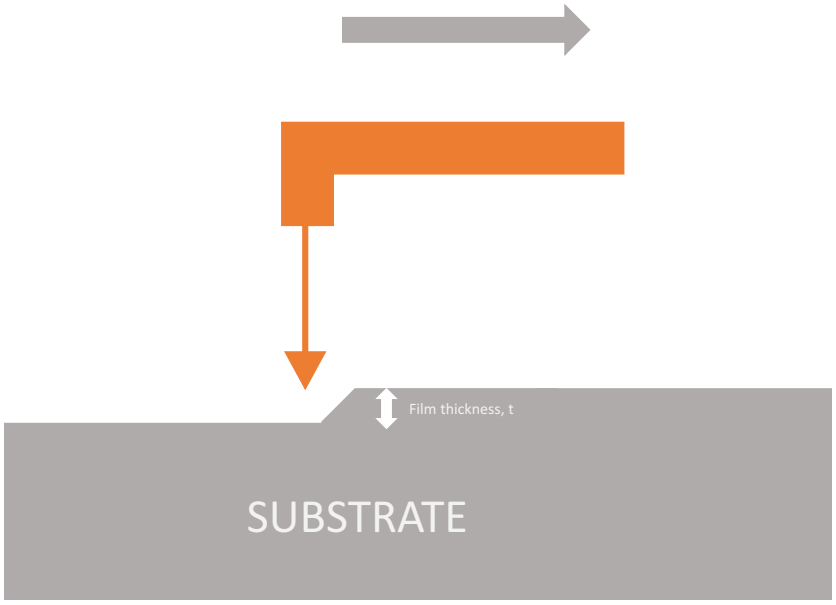


Figure 3: Profilometer.

### 3.5.4 XRF

X-ray Fluorescence spectrometer (XRF) was used to measure the compositions of tungsten and indium. From XRF you can determine the chemistry of a sample. The material is bombarded with high energy primary X-rays. Each element present in the sample emits a set of characteristic fluorescent (or secondary) X-rays. This X-ray is unique for that specific element which can be measured and analyzed to find out what elements are present in the sample. XRF spectroscopy is an excellent technology for qualitative and quantitative analysis of material composition. The unit is cps/mA, where cps means counts per second [11].

### 3.5.5 XRD

X-ray diffraction (XRD) is a method to determine the crystallographic structure of a material. When monochromatic X-rays are scattered from a substance with a structure on this scale, it causes interference. The detector counts the number of X-rays observed at each angle 2 theta. This angle is used since it is the angle between incident and reflected X-ray, due to Bragg's law. XRD measurement leads to a pattern of lower and higher intensity. With crystals, the model generates three-dimensional diffraction chips that respond to X-ray wavelengths, like the spacing of planes in a crystal lattice. This process is called constructive interference and is used as a technique to study crystal structure and atomic spacing. All diffraction methods begin with emitting X-rays focused on a sample. These scattered X-rays are collected and you can then analyze the structure of the sample is analyzed. This

is possible because each mineral has a unique diffraction pattern [4].

### 3.5.6 GDOES

Glow-discharge optical emission spectroscopy (GDOES) was, in this project, used for detecting hydrogen in the samples to either confirm or dispute the theory about hydrogen affecting the conductivity in the undoped indium oxide samples. GDOES is a method for the quantitative analysis of metals and other nonmetallic solids. The samples are used as a cathode in either a DC or AC current plasma. From the surface, the sample is sputtered with argon ions to remove the layers. The atoms that are removed diffuses into the plasma. Then, elements emit excited waves which have characteristic wavelengths. These waves are recorded by a downstream spectrometer and then quantified. An element spectrum is presented after the measurement [12].

### 3.5.7 SEM

Scanning electron microscope (SEM) was used, mostly to validate the thicknesses measured with the profilometer, but also to analyze the microstructure of the film. SEM is a type of electron microscope where you get an image of a sample by scanning the surface with a focused beam of electrons. The electrons interact with the atoms in the sample. This generates various signals containing information about the surface topography and composition of the sample. The electron beam is scanned in a raster fashion, and the position of the beam is combined with the detected signal strength to produce an image. Some SEMs can achieve resolutions greater than one nanometer. The signals used by the SEM to generate the images result from the interaction of the electron beam with atoms at different depths in the sample. Different types of signals are generated including secondary electrons, reflected or backscattered electrons, characteristic x-rays and light (cathode luminescence), absorbed current (sample current) and electrons transferred. In this work, a secondary electron detector was used for cross-sectional imaging and energy dispersive X-ray spectroscopy for compositional analysis [13].

# 4 Results & Discussion

In this section all the results, with the following discussion, are presented from the first and second batch of depositions.

## 4.1 First batch of depositions

The results from the first depositions without tungsten are presented in table 1.

Table 1: The sheet resistance of the first batch of depositions without tungsten, sorted by the flow of oxygen.

| Sample | $O_2[sccm]$ | $P_W[W]$ | $R_s[\Omega/sq.]$ |
|---|---|---|---|
| IOW13 | 0 | 0 | $1.93 \cdot 10^2$ |
| IOW03 | 0.2 | 0 | $4.55 \cdot 10^1$ |
| IOW08 | 0.3 | 0 | $5.92 \cdot 10^1$ |
| IOW07 | 0.5 | 0 | $8.00 \cdot 10^4$ |

After the first depositions without tungsten an optimal oxygen gas flow was found to be around 0.2 - 0.3 sccm. This was decided by measuring the sheet resistance of the samples in table 1 and finding a minimum in sheet restistance as a function of oxygen gas flow. This showed that lower oxygen gas flow resulted in higher sheet resistance, and also increasing the oxygen gas flow even more from 0.3 sccm, increased the sheet resistance (see figure 4). That justified the choice of oxygen gas flow for the following depositions.

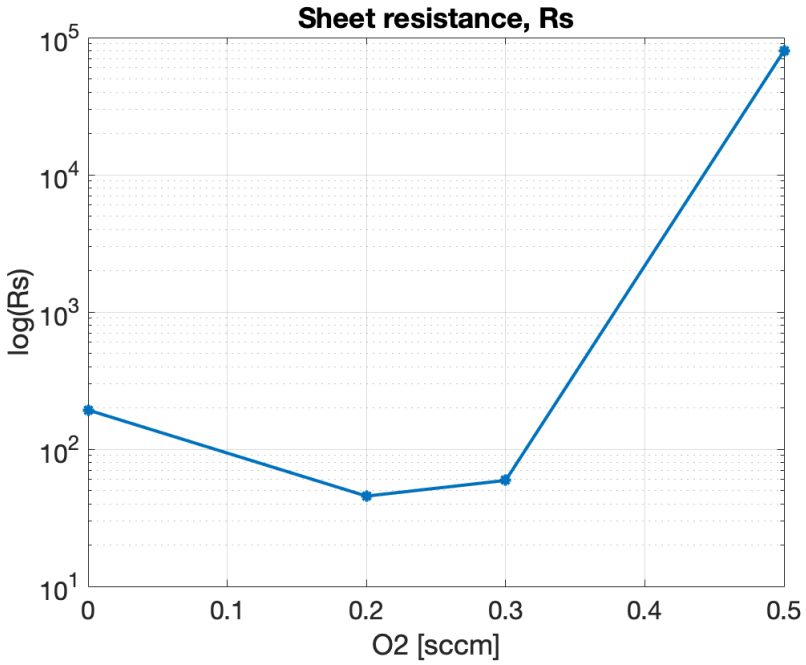


Figure 4: Logaritmic scale of sheet resistance from table 1 with altered oxygen flow and zero tungsten power.

With the knowledge of optimal oxygen gas flow, tungsten was added in the process. In table 2 the samples of depositions from the first batch, with tungsten, are listed. When looking at the results, from both with and without tungsten, the lowest sheet resistance reached was 4.55 $\cdot 10^1$ $\Omega$/sq. This was for sample IOW03 with 0 W tungsten. The lowest sheet resistance with tungsten was reached in sample IOW16 and was 3.66 $\cdot 10^2$ $\Omega$/sq.

Table 2: The sheet resistance of the first batch of depositions with tungsten, sorted by the tungsten power.

| Sample | $O_2[sccm]$ | $P_W[W]$ | $R_s[\Omega/sq.]$ |
|---|---|---|---|
| IOW16 | 0.3 | 3 | 3.66 $\cdot 10^2$ |
| IOW17 | 0.5 | 3 | 4.85 $\cdot 10^3$ |
| IOW11 | 0.3 | 15 | 6.50 $\cdot 10^3$ |
| IOW15 | 0.8 | 15 | 2.08 $\cdot 10^3$ |
| IOW09 | 0.3 | 20 | 2.21 $\cdot 10^3$ |
| IOW10 | 0.5 | 20 | 5.76 $\cdot 10^2$ |
| IOW12 | 0.8 | 20 | 5.76 $\cdot 10^7$ |

The samples IOW09, IOW10, IOW11 and IOW13 came out dark (see example of IOW09 in figure 16c in Appendix) and had very high sheet resistance. IOW12 was a bit more transparent but had by far the highest sheet resistance of $5.76 \cdot 10^7$ $\Omega$/sq. This behaviour can be explained as follows: Increasing oxygen flow can oxidize the tungsten but instead the films get completely oxidized and thus insulating. Other samples came out very resistive, for example IOW12. This sample is the one with the highest oxygen gas flow, and also highest tungsten power which, according to theory and analyzes in this project, explains the high sheet resistance. The ratio of tungsten plus indium to oxygen determines transparency and metallicity. More tungsten with low oxygen flow can lead to metallicity. Adding more oxygen to that leads to more tranparency due to oxygen oxidizing the tungsten. A coating of tungsten oxide is then made, rather than with the metal tungsten and indium.

The figures 5, 6 and 7 show the results from the optical measurements, transmittance, reflectance and absorptance. Only IOW08, IOW09, IOW11, IOW16 and IOW17 were measured from the first batch. IOW08 was chosen because it was one of the undoped samples. IOW09 and IOW11 were chosen because they were dark and for comparison, they were interesting to include in the measurements. IOW16 and IOW17 were included since they were deposited in a modified deposition process where the power on the W target was reduced using pulsed magnetron sputtering.

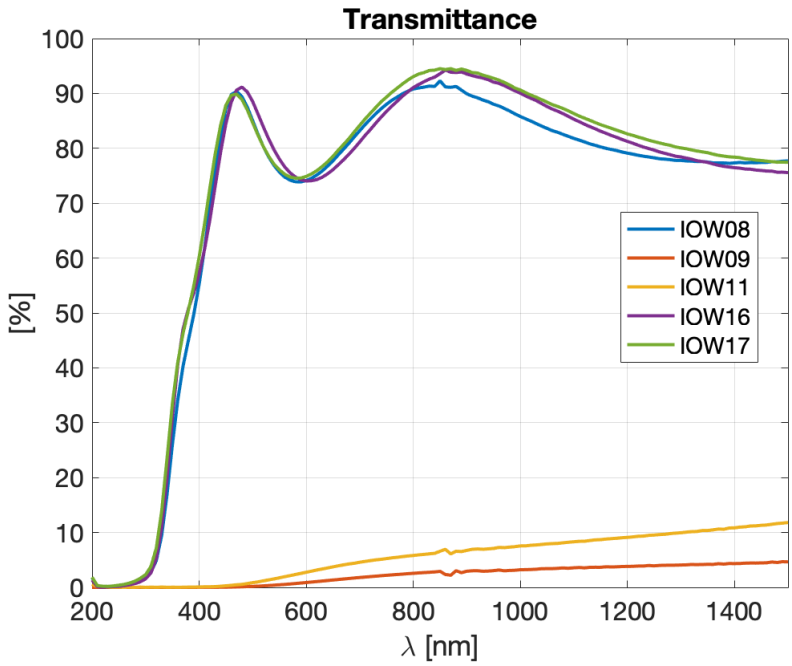


Figure 5: Transmittance for the samples in first batch of depositions.

Figure 5 shows the transmittance for the measured samples. As seen, IOW08, IOW16 and IOW17 follow the same path for transmittance while IOW09 and

IOW11 have low transmittance in the entire spectral range. This was expected, since IOW09 and IOW11 were two of the dark samples which then reasonably have lower transmittance.

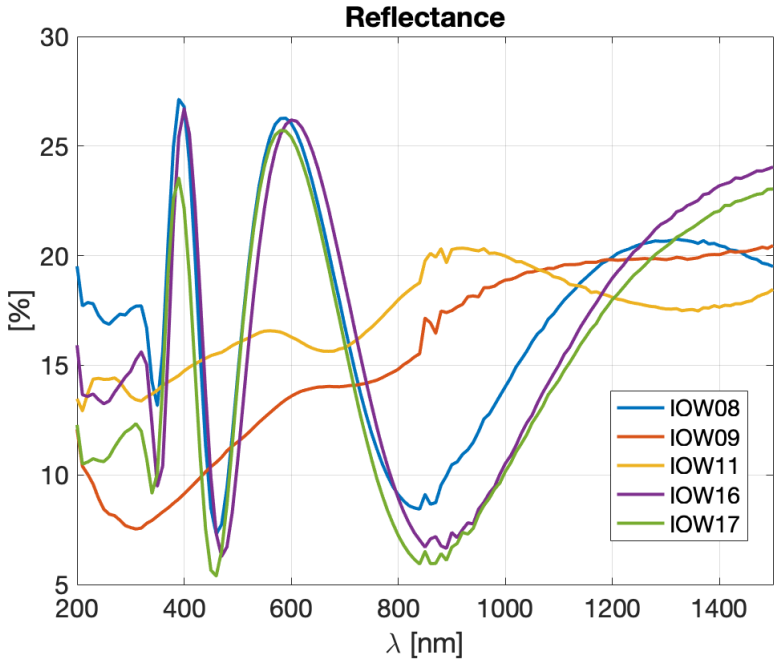


Figure 6: Reflectance for the samples in first batch of depositions.

From figure 6, the reflectance can be compared. IOW16 and IOW17 follow the same path. IOW08 is almost the same as IOW 16 and IOW17, but for longer wavelengths IOW08 has lower reflectance, while IOW09 and IOW11 have somewhat higher and even reflectances through all the wavelengths. These samples absorb more light and since they were not as transparent as the other measured samples, but not completely dark either, the results are reasonable according to equation 2.

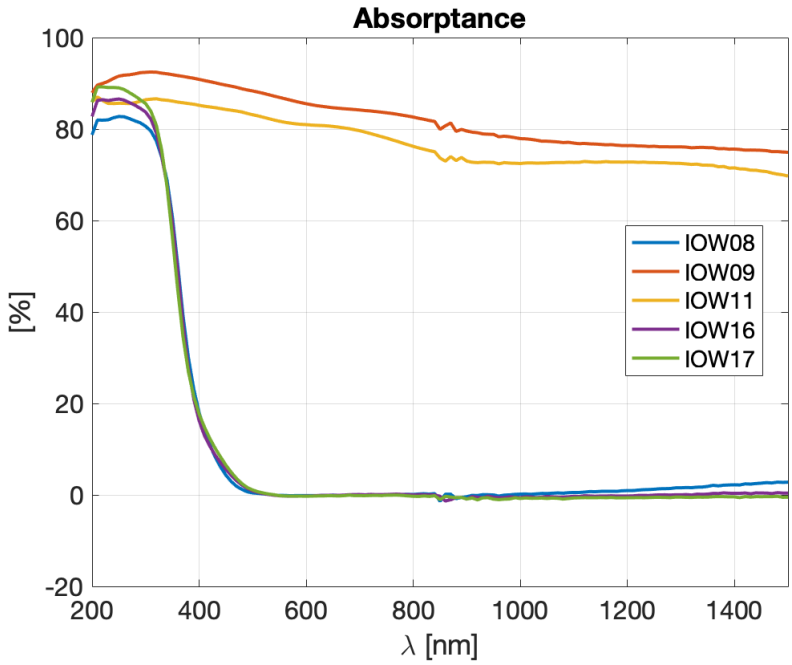


Figure 7: Absorptance for the samples in first batch of depositions.

As seen in figure 7, samples IOW09 and IOW11 are opaque. These samples were two of the ones that got dark and not transparent. The other samples absorb a lot of light for short wavelengths but almost zero % from 500 nm, below the band gap.

These results can be compared to the literature. IOW08, IOW16 and IOW17 achieves expected results for transmittance, reflectance and absorptance since they were transparent, whereas IOW09 and IOW11 deviates from literature since they were opaque. The tungsten doped films, IOW16 and IOW17 have lower absorptance than the undoped IOW08, for longer wavelengths.

The thickness was measured to calculate the resistivity from the sheet resistance measurements. The results are presented in table 3.

Table 3: Results from the measurements with profilometer and 4-point probe, sorted by the tungsten power.

| Sample | $O_2[sccm]$ | $P_W[W]$ | Thickness [nm] | Resistivity [$\Omega cm$] |
|---|---|---|---|---|
| IOW13 | 0 | 0 | 188 | $3.60 \cdot 10^{-3}$ |
| IOW03 | 0.2 | 0 | 140 | $6.36 \cdot 10^{-4}$ |
| IOW08 | 0.3 | 0 | 242 | $1.40 \cdot 10^{-3}$ |
| IOW07 | 0.5 | 0 | 195 | $1.56 \cdot 10^{0}$ |
| IOW16 | 0.3 | 3 | 225 | $8.20 \cdot 10^{-3}$ |
| IOW17 | 0.5 | 3 | 165 | $8.01 \cdot 10^{-2}$ |
| IOW11 | 0.3 | 15 | 188 | $1.22 \cdot 10^{-1}$ |
| IOW 15 | 0.8 | 15 | 279 | $5.81 \cdot 10^{-2}$ |
| IOW09 | 0.3 | 20 | 304 | $6.72 \cdot 10^{-2}$ |
| IOW10 | 0.5 | 20 | 260 | $1.50 \cdot 10^{-2}$ |
| IOW12 | 0.8 | 20 | 219 | $1.26 \cdot 10^{3}$ |

The lowest resistivity reached was $6.36 \cdot 10^{-4}\Omega$cm. This was for sample IOW03 with 0 W tungsten. According to literature, IOW can reach a resistivity on the order of $10^{-4}\Omega$cm. The lowest resistivity reached with tungsten was for sample IOW16 and the resistivity was $8.20 \cdot 10^{-3}\Omega$cm. As seen, the film thickness varies a lot between the samples. It is strange since the deposition times were the same for all the samples. This is discussed later in the section.

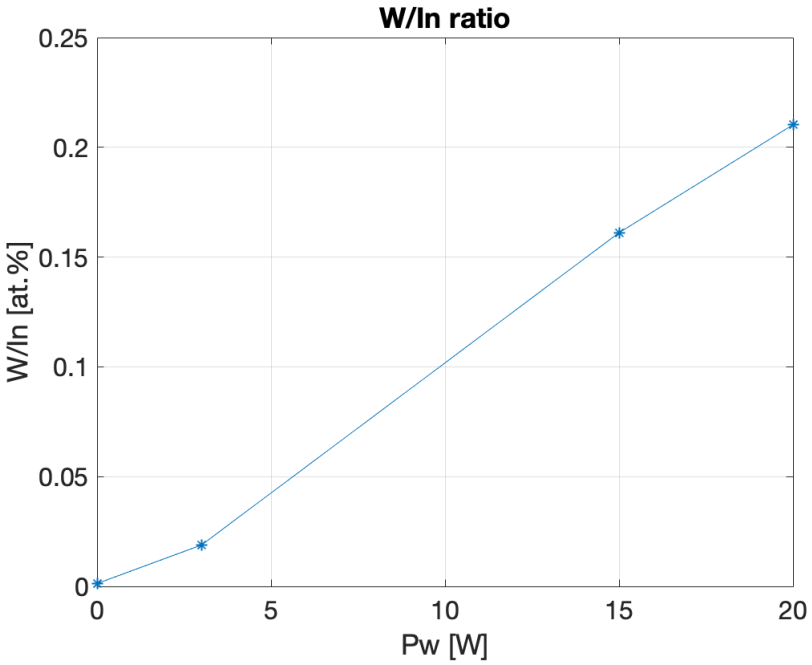


Figure 8: W to In ratio from values in table 4

Figure 8 shows the results from XRF and the tungsten content related to indium content. The figure shows a quite linear connection between the tungsten power and the amount of tungsten to indium in the film. The figure was plotted from the data in table 4, subtracting the reference values, and also calibrated against the SEM measurement. The reference used in the measurements was a piece of quartz glass since the thin film was coated on quartz glass. As seen in the table the intensity of the tungsten peak for IOW08 is not zero, although no tungsten is in the thin film. That is the reason for the reference measurement. The intensity of the tungsten peak is almost the same in the reference as for IOW08 which means, as expected, that no tungsten is present in IOW08. The intensity of the indium peak is fairly constant for all the samples. This indicates that the amount of indium was comparable in all depositions, contradicting the measured thicknesses in the profilometer. The results show that this approach is suitable for deposition of films with controlled tungsten content because the tungsten can be adjusted in a wide range.

Table 4: Results from XRF.

| Sample | Indium [cps/mA] | Tungsten [cps/mA] | W/In ratio [at.%] |
|---|---|---|---|
| Reference | 9.2 | 7.0 | - |
| IOW 08 | 301.2 | 7.5 | 0.13 |
| IOW 09 | 316.6 | 90.8 | 21.03 |
| IOW 11 | 311.2 | 70.1 | 16.11 |
| IOW 16 | 303.4 | 14.1 | 1.88 |

Results from XRD measurements are shown in figure 9. In the figure you can see a number of sharp peaks which indicates a crystalline structure in the films for IOW08 and IOW16. All peaks in Theta-2theta (T2T) corresponds to indium oxide phase. The samples with much tungsten, IOW09 and IOW11 have many peaks corresponding to tungsten and are therefore not crystalline. The diffractogram shows there are no metallic tungsten in any of the measured samples, even the tungsten rich films. The reflections shows something close to tungsten trioxide or any other suboxide.

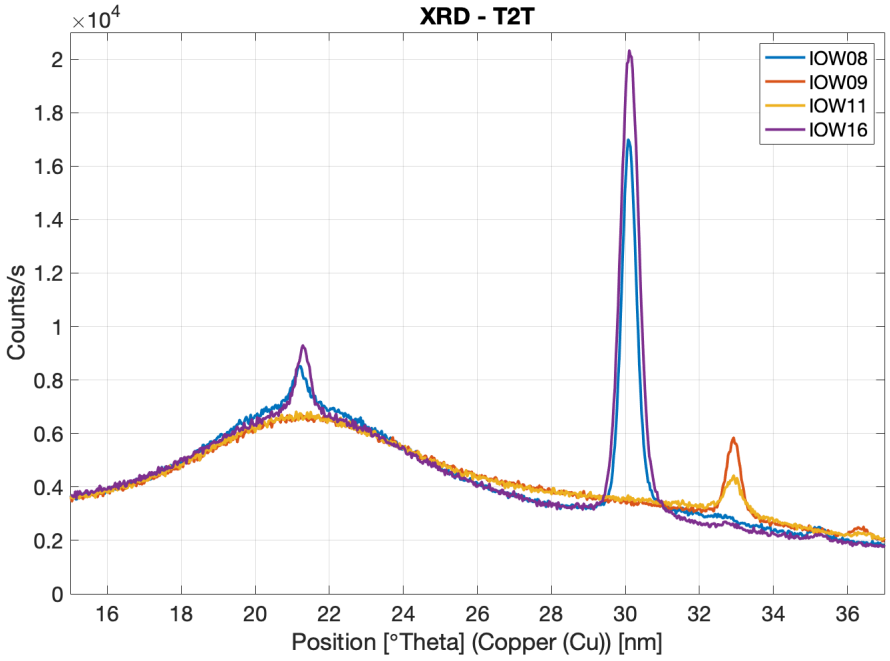


Figure 9: Results from XRD measurements, Theta-2theta (T2T).

Overall, the results from the first batch varies a lot. Some of the samples came out very dark and not so transparent while some meet the expected transmittance for a TCO. When it comes to the resistivity the lowest resistivity reached was for the undoped sample. The lowest resistivity for IOW sample was still not low enough to perform as a TCO in a thin film solar cell when comparing to literature.

## 4.2 Second batch of depositions

In the second batch, pulsed magnetron sputtering was used to keep the tungsten content low. The samples from the second batch are listed in table 5. As seen, the lowest resistivity reached was 1.00 $\cdot 10^{-3}\Omega$ cm and also in this batch, it was the undoped sample which had the lowest resistivity. The lowest resistivity reached with tungsten was for sample IOW18 and was 6.50 $\cdot 10^{-3}\Omega$ cm. In this batch all samples were transparent. One interesting observation is that IOW18 is better than IOW19 even though IOW18 has a higher tungsten power. It could be that the optimum tungsten concentration is closer to IOW19 or there might be due to measurement errors in the 4-point probe.

Table 5: Results from second batch of depositions with and without tungsten.

| Sample | $O_2[sccm]$ | $P_W[W]$ | $R_s[\Omega/sq.]$ | Thickness [nm] | Resistivity $[\Omega cm]$ |
|---|---|---|---|---|---|
| IOW18 | 0.3 | 3 | $4.03{\cdot}10^{2}$ | 161 | $6.50{\cdot}10^{-3}$ |
| IOW19 | 0.3 | 1.5 | $7.71 \cdot 10^{2}$ | 170 | $1.31{\cdot}10^{-2}$ |
| IOW20 | 0.3 | 0 | 56.0 | 187 | $1.00{\cdot}10^{-3}$ |

Figures 10, 11 and 12 show the optical properties for the second batch of depositions. In this batch, all samples were transparent and therefore optical measurements were made on all of them.

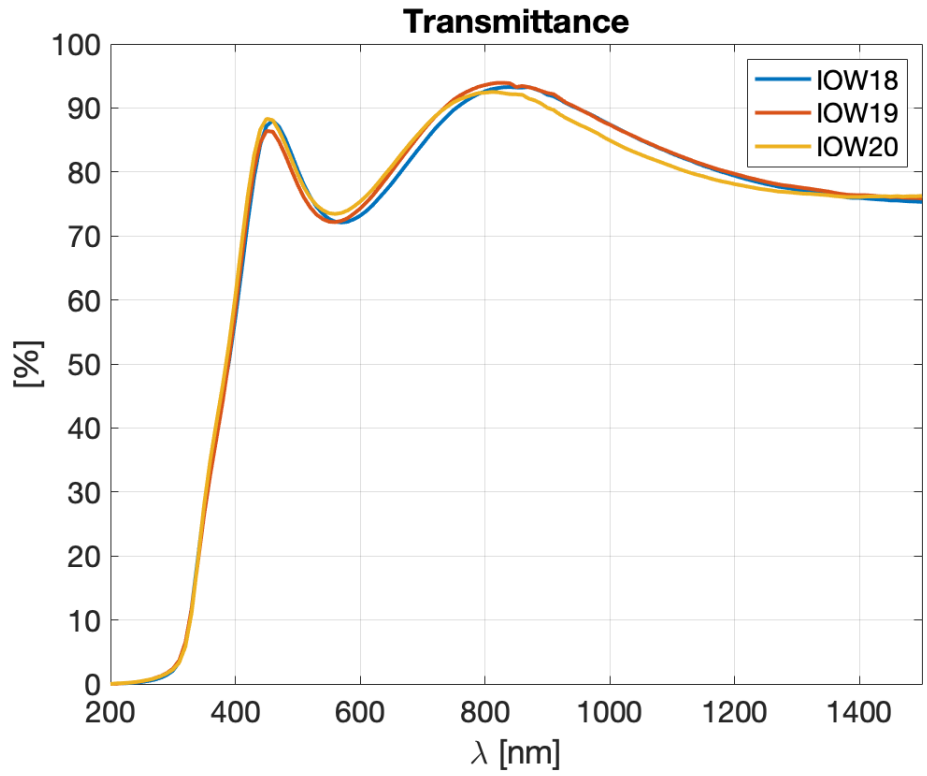


Figure 10: Transmittance for the samples in second batch of depositions.

From figure 10, the transmittance can be compared. As seen in the results, these samples all have a high transmittance, around 90 % for some wavelengths. All samples follow the same path and therefore have almost the same transmittance through all wavelengths. It was expected that the different samples had high transmittance due to the transparent films.

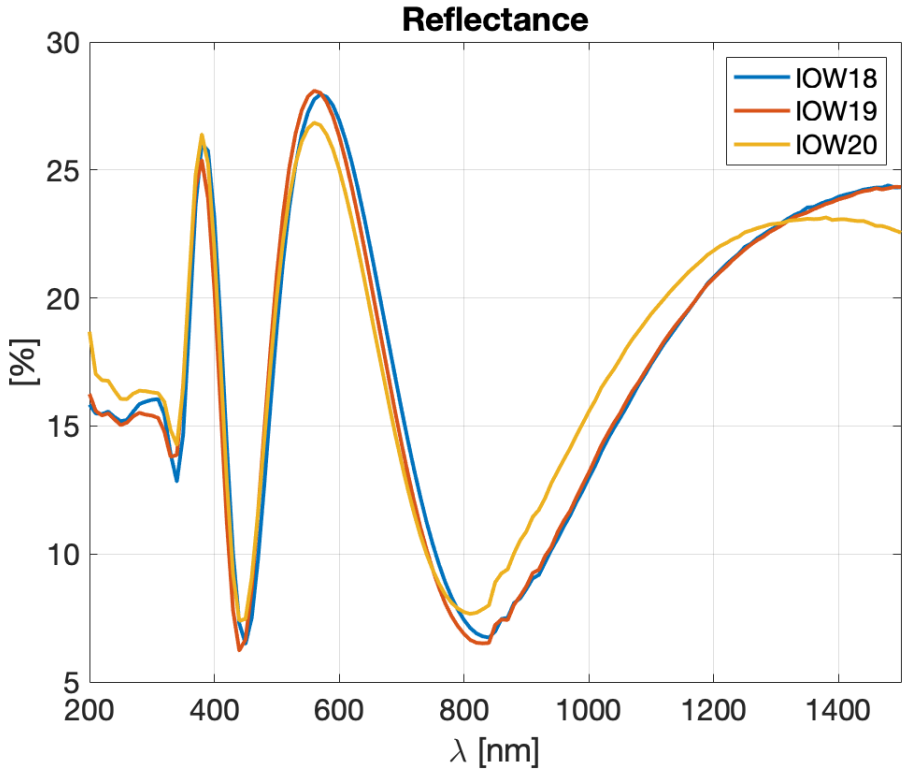


Figure 11: Reflectance for the samples in second batch of depositions.

Figure 11 shows the reflectance for all the samples. Also here, all samples follow the same path, except for a small difference for longer wavelengths, IOW20 differs slightly from the others. IOW20 is the undoped sample which could explain some small differences in the graph.

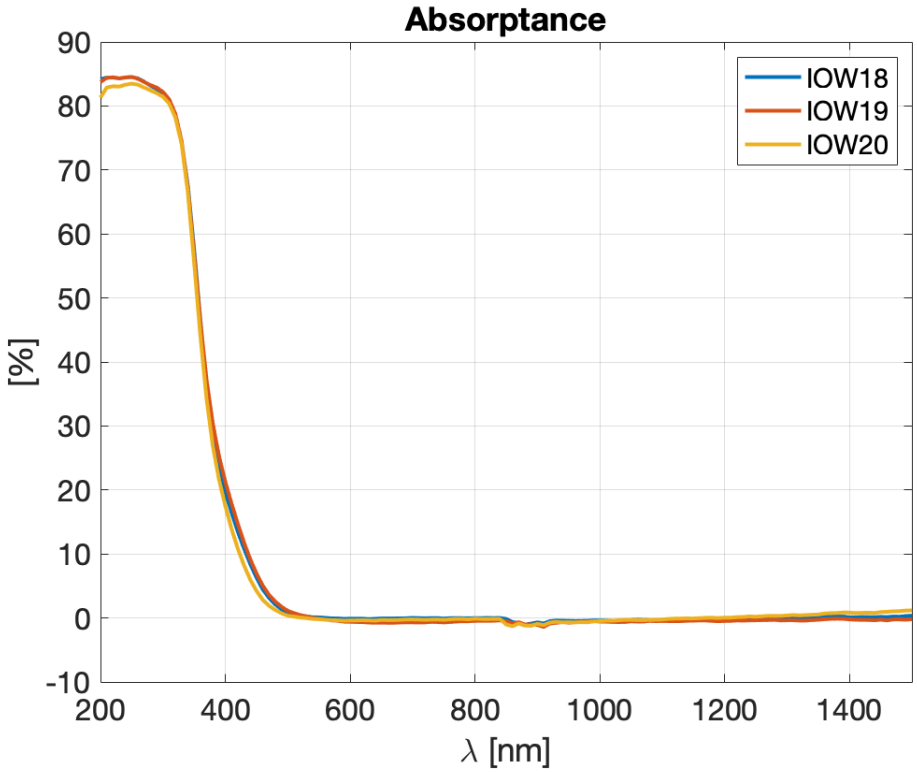


Figure 12: Absorptance for the samples in second batch of depositions.

Figure 12 shows the absorptance. All samples follow the same path and therefore have almost the same absorptance through all wavelengths. They absorb a lot of light for shorter wavelengths and almost zero from around 500 nm. All three samples are, as mentioned, transparent and therefore it is expected to have low absorptance.

All three samples achieves expected results for transmittance, reflectance and absorptance, according to literature.

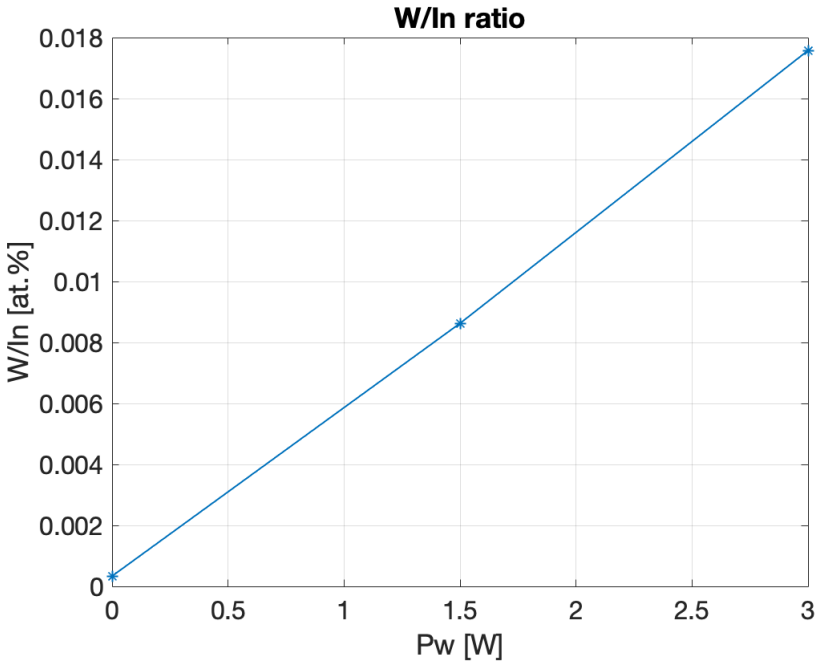


Figure 13: W to In ratio.

The measurement of tungsten to indium ratio shows, also for this batch, that it is directly proportional to the tungsten power (see Figure 13). In table 6 the data used for the figure are listed. The same reference (quartz glass) as in the first batch was used for these samples which means the reference values from table 4 were subtracted from the values in table 6.

Table 6: Results from XRF.

| Sample | Indium [cps/mA] | Tungsten [cps/mA] | W/In ratio [at.%] |
|---|---|---|---|
| IOW 18 | 261.6 | 12.7 | 1.76 |
| IOW 19 | 277.3 | 10.0 | 0.86 |
| IOW 20 | 286.0 | 7.1 | 0.03 |

Measurements with scanning electron microscope (SEM) were made on some samples (IOW03, IOW09, IOW16 and IOW18) to validate the thickness measurements with profilometer. This was because of unexpected differences in film thickness from both the first and second batch. Since deposition time was the same for all samples, the thickness of the samples should be somewhat similar. However, this was not the case according to the profilometer measurements. In the profilometer you set the

levels in the profile of the thin film. This part is important for the final results of the measurements and probably where some errors could have appeared. Judging from the fact that the SEM measurements did not confirm the large variations in thickness, the results from profilometry are not reliable.

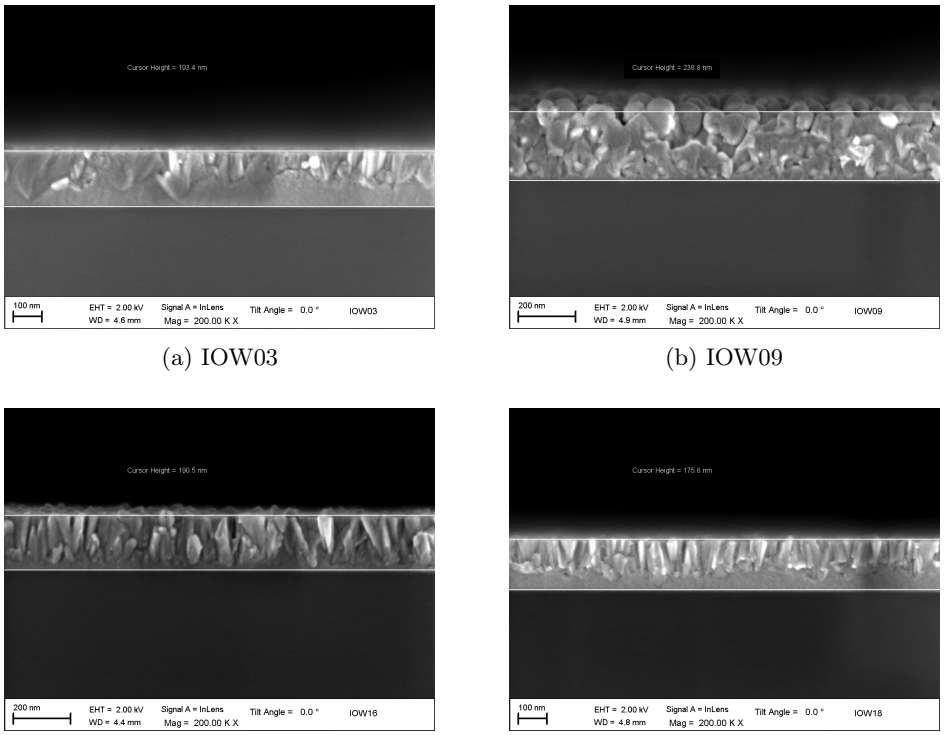


(a) IOW03 (b) IOW09

(c) IOW16 (d) IOW18

Figure 14: Results from the SEM measurements.

When measuring the films, interesting discoveries where made. There seemed to be an amorphous layer in the bottom and grains/columns in the upper 2/3:s of the IOW film (see figure 14). The dark film, IOW09, was very different and porous, but also there were some differences in the structure even between the three transparent layers.

Surprisingly, the undoped films were more conductive than the ones doped with tungsten. It is known that hydrogen doping greatly increases conductivity of $In_2O_3$ [5]. Therefore, Glow-Discharge Optical Emission Spectroscopy measurement was carried out to investigate possible hydrogen incorporation in the studied films. This measurement were made by Jan Keller, researcher at Department of Materials Science and Engineering, Solar Cell Technology at Uppsala University. Figure 15 was given from the measurement. As seen in the figure, the level of hydrogen is higher in the beginning, which means there were hydrogen detected at the surface of the samples. When analyzing deeper into the films, the graph for hydrogen stays constantly around zero. Therefore, it can be concluded that no hydrogen were detected

in the thin films and hydrogen cannot explain the observed results. This finding is further supported by the fact that there was no difference in the resistivity of the two $In_2O_3$ films deposited at very different base pressures.

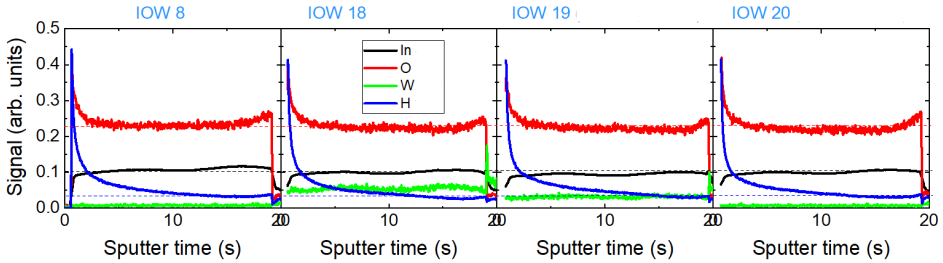


Figure 15: Results from GDOES measurement. No hydrogen detected in the films.

In the second batch all depositions were transparent and have good optical properties. Still the conductivity does not have good enough performance for a TCO. The lowest resistivity was also in this batch for the undoped material. For the IOW the lowest resistivity was in the size of $10^{-3}\Omega$cm. According to theory, doping should lead to higher conductivity [4]. It is likely that tungsten is not active as a dopant in the structure, despite being in the films. The resistivity of the samples can be compared to ITO. ITO has a resistivity in the size of $10^{-4}$ $\Omega$ cm and in this project, onyl the undoped material reached the same size of resistivity. The expected result according to the literature, is that tungsten doped indium oxide should have good conductivity and good optical properties. The samples from this project does unfortunately not meet all of those requirements [1].

## 4.3 Suggested improvements

One challenge was getting low enough tungsten content. The pulsed power approach was shown to provide a reliable means for controlling the tungsten content down few at. %. However, the doped samples were still worse than the undoped when it comes to electrical conductivity, which means other post-treatments of the samples might have been necessary to improve the samples.

One thing that could have been done to improve the conductivity was to anneal the samples afterwards. According to the literature reviewed earlier, the optimum tungsten concentration is about 3 % and resistivity on the order of $10^{-4}$ $\Omega$cm can the be achieved. Thermal treatment, however, may be necessary to achieve the best possible performance [3]. The results achieved in this project are about 10 times worse, indicating the need for further annealing. This is also in agreement with the observed microstructure where at least part of the film appears to be amorphous. Annealing would crystallize the films even more and improve the electrical conductivity.

# 5 Conclusion

According to the aim of this project some conclusions can be made. Although other studies show that IOW in fact can reach desired properties for a TCO in thin film solar cells, these required values were not achieved in this project. Using this manufacturing process can not lead to IOW thin films, with good enough electrical performances. The lowest resistivity reached was still too high for a TCO. The low amount of tungsten desired was not able to be achieved using RF magnetron sputtering. Using pulsed magnetron sputtering gave lower tungsten content, still the resistivity was too high. Something that could be tested in the future could be to use tungsten trioxide target instead of metal tungsten target. Post-treatments, like annealing, could be another thing to improve the IOW thin films to crystallize the films and increase the electrical conductivity.

The optical performances for several of the samples were suitable for a TCO, with high transmittance and low absorptance. Some samples, with high tungsten sputtering power, came out dark and had high absorbance. The transmittance for the IOW films reached the same level as existing materials, such as AZO or ITO, still the IOW thin films made in this project can not yet replace these materials, due to the worse electrical conductivity.

However, tungsten doped indium oxide has high potential to replace these materials in the future, with further investigations and development of the deposition process and material characterization.

# References


[1] Sebastian C Dixon et al. "n-Type doped transparent conducting binary oxides: an overview". In: *Journal of Materials Chemistry C* 4.29 (2016), pp. 6946–6961.

[2] Ivan G Samatov et al. "Room-temperature rf-magnetron sputter-deposited W-doped indium oxide: decoupling the influence of W dopant and O vacancies on the film properties". In: *Applied Physics A* 122.4 (2016), pp. 1–10.

[3] Fanying Meng et al. "High mobility transparent conductive W-doped In2O3 thin films prepared at low substrate temperature and its application to solar cells". In: *Solar energy materials and solar cells* 122 (2014), pp. 70–74.

[4] M. Ohring. *The materials science of thin films. Chapter 3, 6 11.* 79-545. London: Academic Press, 1992.

[5] Timo Jäger et al. "Hydrogenated indium oxide window layers for high-efficiency Cu (In, Ga) Se2 solar cells". In: *Journal of Applied Physics* 117.20 (2015), p. 205301.

[6] Yuanpeng Zhang et al. "Effects of dopant content on optical and electrical properties of In2O3: W transparent conductive films". In: *Rare Metals* 31.2 (2012), pp. 168–171.

[7] Wan Joo Maeng et al. "Highly conducting, transparent, and flexible indium oxide thin film prepared by atomic layer deposition using a new liquid precursor Et2InN (SiMe3) 2". In: *ACS applied materials & interfaces* 6.20 (2014), pp. 17481–17488.

[8] Ram K Gupta et al. "High mobility W-doped In2O3 thin films: Effect of growth temperature and oxygen pressure on structural, electrical and optical properties". In: *Applied Surface Science* 254.6 (2008), pp. 1661–1665.

[9] Jiaojiao Pan et al. "Tungsten doped indium oxide thin films deposited at room temperature by radio frequency magnetron sputtering". In: *Journal of Materials Science & Technology* 30.7 (2014), pp. 644–648.

[10] Robert Derek Arnell, PJ Kelly, and JW Bradley. "Recent developments in pulsed magnetron sputtering". In: *Surface and Coatings Technology* 188 (2004), pp. 158–163.

[11] Krishna Seshan. *Handbook of thin film deposition*. William Andrew, 2012.

[12] Thomas Nelis and Richard Payling. *Glow discharge optical emission spectroscopy: a practical guide*. Vol. 7. Royal Society of Chemistry, 2003.

[13] Azad Mohammed and Avin Abdullah. "Scanning electron microscopy (SEM): A review". In: *Proceedings of the 2018 International Conference on Hydraulics and Pneumatics—HERVEX, Băile Govora, Romania*. 2018, pp. 7–9.

# 6 Appendix

Table 7: Results from all depositions with and without tungsten, sorted by sample number. Some samples are not included since they where either not measurable or just test samples

| Sample | $O_2[sccm]$ | $P_W[W]$ | $R_s[\Omega/sq.]$ | W/In ratio [%] | Thickness [nm] | Resistivity [$\Omega cm$] |
|---|---|---|---|---|---|---|
| IOW03 | 0.2 | 0 | $4.55{\cdot}10^{1}$ | - | 140 | $6.36{\cdot}10^{-4}$ |
| IOW07 | 0.5 | 0 | $8.00{\cdot}10^{4}$ | - | 195 | $1.56{\cdot}10^{0}$ |
| IOW08 | 0.3 | 0 | $5.92{\cdot}10^{1}$ | 0.13 | 242 | $1.40{\cdot}10^{-3}$ |
| IOW09 | 0.3 | 20 | $2.21{\cdot}10^{3}$ | 21.0 | 304 | $6.72{\cdot}10^{-2}$ |
| IOW10 | 0.5 | 20 | $5.76{\cdot}10^{2}$ | - | 260 | $1.50{\cdot}10^{-2}$ |
| IOW11 | 0.3 | 15 | $6.50{\cdot}10^{3}$ | 16.1 | 188 | $1.22{\cdot}10^{-1}$ |
| IOW12 | 0.8 | 20 | $5.75{\cdot}10^{7}$ | - | 219 | $1.26{\cdot}10^{3}$ |
| IOW13 | 0 | 0 | $1.93{\cdot}10^{2}$ | - | 188 | $3.60{\cdot}10^{-3}$ |
| IOW15 | 0.8 | 15 | $2.08{\cdot}10^{3}$ | - | 279 | $5.81{\cdot}10^{-2}$ |
| IOW16 | 0.3 | 3 | $3.66{\cdot}10^{2}$ | 1.88 | 225 | $8.20{\cdot}10^{-3}$ |
| IOW17 | 0.5 | 3 | $4.85{\cdot}10^{3}$ | - | 165 | $8.01{\cdot}10^{-2}$ |
| IOW18 | 0.3 | 3 | $4.03{\cdot}10^{2}$ | 1.76 | 161 | $6.50{\cdot}10^{-3}$ |
| IOW19 | 0.3 | 1.5 | $7.71{\cdot}10^{2}$ | 0.86 | 170 | $1.31{\cdot}10^{-2}$ |
| IOW20 | 0.3 | 0 | $5.56{\cdot}10^{1}$ | 0.03 | 187 | $1.00{\cdot}10^{-3}$ |

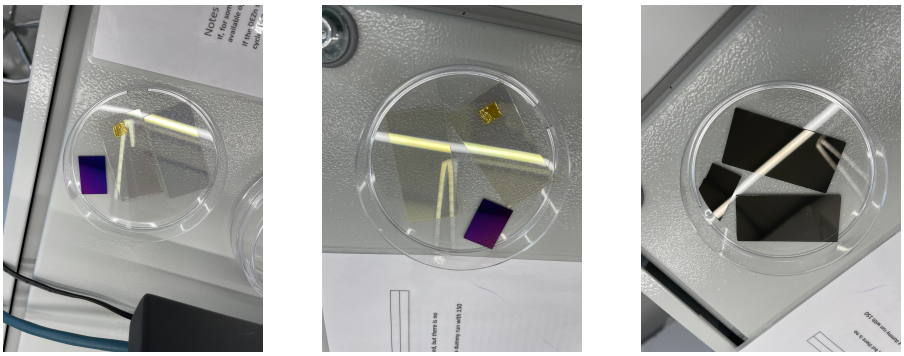

(a) IOW03 (b) IOW08 (c) IOW09

Figure 16: Example of how the samples looked.

(a) The sputtering machine (b) Chamber during deposition (c) Chamber during deposition

Figure 17: Picture of the sputter and chamber during deposition